Journal of Materials and Electronic Devices 1 (2019) 55-59

Elasticalorimetric Shape Memory Alloy Systems and The Effect of Pressure on Characteristic Properties of SMAs

C. Aksu Canbay[1,*], M.A. Çiçek[2], A. Odabaşi[3]

[1]Firat University, Faculty of Science, Department of Physics, Elazig/Turkey
[2]Firat University, Kovancılar Vocational School, Departmentof Opticianary, Elazig/Turkey
[3]Firat University, Engineering Faculty, Department of Metallurgy and Material Engineering, Elazig/Turkey

Shape memory alloys are the materials that can gain its original shape after the deformation caused by heat, pressure or magnetic field. In this work, we investigated the pressure effect on the characteristic phase transformation temperatures, order-disorder phase transitions and also the effect on morphology. Kinetic parameters were detected by thermal analysis results and activation energy variation was calculated. The morphological analyses were made at room temperature by XRD and optical microscope analysis then the alterations in diffraction patterns were detected.

Keywords: Cu-based shape memory alloys, Martensitic transformation, Shape memory effect, Pressure.

Submission date:01 October 2019
Acceptance Date:28 November 2019

**Corresponding authors*:caksu@firat.edu.tr

1. Introduction

In recent years, with the advances in technology, smart materials became widely used in numerous different modern technological and industrial fields from actuator, aerospace, automotive to medical, robotics, so on. Shape memory alloys (SMAs) are among the most widely used smart materials [1-3]. SMAs vary widely in applications and frequently used in industrial and medical moments due to their very useful special properties such as shape memory effect (SME), superelasticity (SE), high damping ability and corrosion resistance[4, 5].

SMAs exhibit their extraordinary ability to switch from the existing solid crystal structure to a different solid crystal form by the applied external physical factors such as heat, stress, electrical field etc.. In general, such materials can be deformed plastically when the temperature is low and return to their structural state prior to deformation when subjected to excess temperatures. This event happens by such a phase change known as martensitic transformation bring in these alloys a macro-scale shape change ability called as shape memory effect (SME) property.

SMAs are generally grouped in three constitutive alloy systems: NiTi, Cu-rich and Fe-rich alloys in the alloy forms of binary, ternary or more [3, 7, 8]. Cu-based SMAs are less expensive and can be produced less difficultly than the famous and superior NiTi ones but they show better SE and SME properties than Fe-based SMAs do. Mostly the Cu-rich SMAs are built on the binary forms of Cu-Al, Cu-Sn and Cu-Zn alloys which can have better SMA properties by doping minor additions of a third or more elements (such as Ni, Mn, Ti, Zr, Be, Fe, Sn, Zn, Cr etc.) that are frequently used as grain refiner to enhance ductility, improve SME and thermal stabilization in these alloys [6-8].

The SME effect in Cu-Al-Ni alloys is also caused by this kind of atomically diffusionless reversible thermoelastic martensitic transformations [8-10]. Cu-Al-Ni SMAs are used frequently due to their inexpensive fabrication cost and high resistance to the degradation of functional properties that occurred by the aging processes and also these alloys can have fairly high transformation temperatures [11]. The improved thermodynamic stability and a wide range of high transformations temperatures above 100 °C are characteristic faculties of Cu-Al-Ni alloys that have atracted researchers, but the applicability of these alloys is limited due to their brittle nature because of their coarse grained polycrystalline, which is caused by a strong elastic anisotropy and the precipitation of certain intermetallic phases [12-15].

In this study, different pressures were applied to Cu-Al-Ni shape memory alloy and according to the applied

pressure value the variation in kinetic parameters and morphology were investigated.

2. Experimental details

Cu-Al-Ni shape memory alloy was fabricated by arc melting method. The composition of the alloy was determined as Cu-13.46Al-4.51Ni (wt.%) by Bruker Model energy dispersive X-ray (EDX).The samples were cut from the ingot and homogenized at β-phase region. Then 280 MPa, 560, MPa, 840 MPa and 1120 MPa pressure was applied on these samples. The characteristic transformation temperatures and thermodynamic parameters of the homogenous and pressure applied samples were determined by Shimadzu DSC-60A differential scanning calorimetry with different heating/cooling rates. The TG/DTA (Shimadzu TA-60 WS) measurements were performed from room temperature to 900 ˚C at a heating rate of 25 ˚C/min. to identify order-disorder phase transitions. X-Ray diffraction patterns of the samples were taken by Rigaku RadB-DMAX II diffractometer and microstructural observations were made using Nikon MA200 model optical metallographic microscope at room temperature.

3. Results and discussion:

The effect of pressure on characteristic high temperature and low temperature phase transformations were detected by Differential scanning calorimetry (DSC) measurements with different heating/cooling rates as; 5, 15, 25, 35 and 45 ˚C/min. and given in Fig. 1-Fig. 5. The transformation temperatures and the hysteresis can be determined by the corresponding peak positions of the DSC measurements so the characteristic transformation temperatures of reverse and forward transformations were determined from DSC curves by tangent method.

The characteristic austenite and martensite phase start and finish temperatures, equilibrium temperatures, enthalpy and entropy values of each sample with different heating/cooling rates are given in Table 1 to Table 4. The equilibrium temperature between the reverse and forward phases according to is determined by the following relation [16];

$$T_0 = \frac{1}{2}\left(M_s + A_f\right) \quad (1)$$

where M_s is the martensite start temperature, A_f is the austenite finish temperature. The entropy change during the reverse transformation can be determined by the following equation [17, 18];

$$\Delta S_{M\rightarrow A} = \frac{\Delta H_{M\rightarrow A}}{T_0} \quad (2)$$

where ΔS is the entropy change, ΔH is the enthalpy change, and T_0 is the equilibrium temperature.

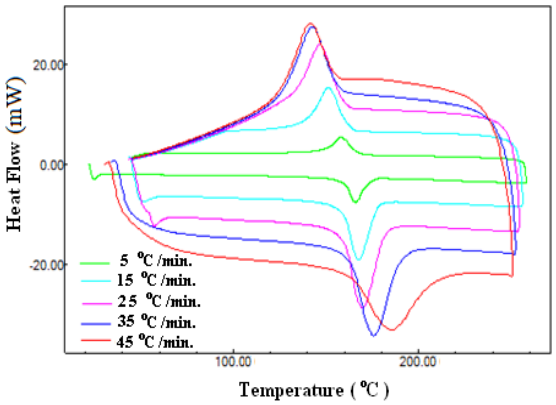

Fig.1: *The DSC curve of the homogenous sample with different heating/cooling rates.*

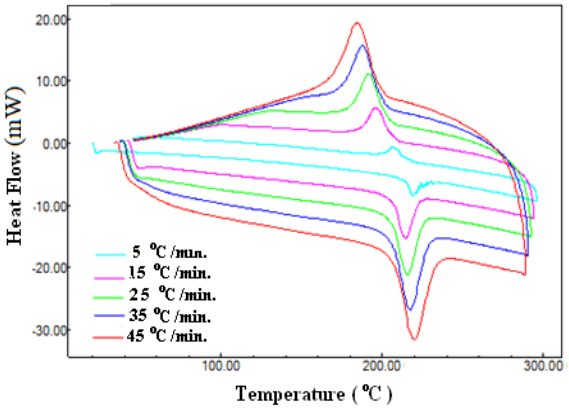

Fig.2: *The DSC curve of the 280 MPa pressure applied sample with different heating/cooling rates.*

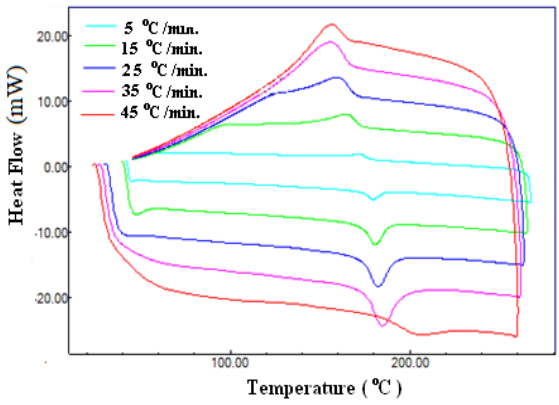

Fig.3: *The DSC curve of the 560 MPa pressure applied sample with different heating/cooling rates.*

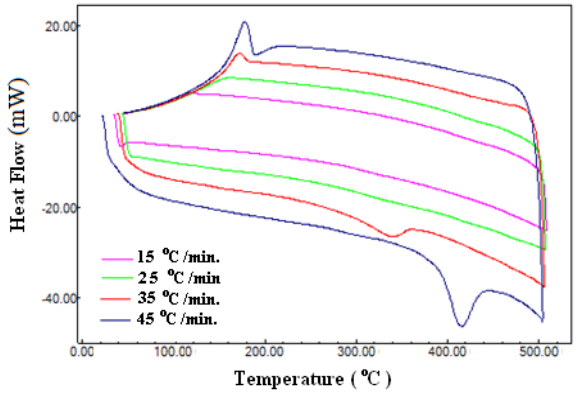

Fig. 4. *The DSC curve of the 840 MPa pressure applied sample with different heating/cooling rates.*

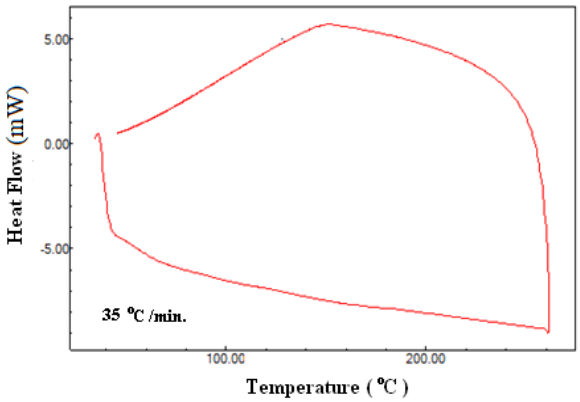

Fig.5: *The DSC curve of the 1120 MPa pressure applied sample with a heating/cooling rate of 35 ˚C/min.*

Table 1: Transformation temperatures and thermodynamic parameters of homogenous sample with different heating/cooling rates (5, 15, 25, 35 and 45 ˚C/min).

Heating/ cooling rate (˚C/min.)	A_s (˚C)	A_f (˚C)	A_{max} (˚C)	T_0 (˚C)	$\Delta H_{M\rightarrow A}$ (J/g)	$\Delta S_{M\rightarrow A}$ (J/g(˚C)	M_s (˚C)	M_f (˚C)	$\Delta H_{A\rightarrow M}$ (J/g)	$\Delta S_{A\rightarrow M}$ (J/g˚C)
5	160.10	171.69	166.32	168.345	11.21	0.066	165.00	150.87	-10.52	-0.062
15	159.84	177.82	167.44	169.52	11.23	0.066	161.22	140.29	-10.94	-0.064
25	159.62	181.54	170.00	170.365	11.46	0.067	159.19	133.88	-12.52	-0.073
35	163.25	190.98	175.97	173.25	10.96	0.063	155.52	127.48	-11.16	-0.064
45	163.88	207.31	185.22	181.34	8.99	0.049	155.37	129.23	-7.61	-0.041

Table 2: Transformation temperatures and thermodynamic parameters of 280MPa pressure applied sample with different heating/cooling rates (5, 15, 25, 35 and 45 ˚C/min).

Heating/ cooling rate (˚C/min.)	A_s (˚C)	A_f (˚C)	A_{max} (˚C)	T_0 (˚C)	$\Delta H_{M\rightarrow A}$ (J/g)	$\Delta S_{M\rightarrow A}$ (J/g(˚C)	M_s (˚C)	M_f (˚C)	$\Delta H_{A\rightarrow M}$ (J/g)	$\Delta S_{A\rightarrow M}$ (J/g˚C)
5	222.76	244.65	219.10	228.905	4.18	0.018	213.16	201.54	-4.28	-0.018
15	207.06	222.69	214.57	214.1	12.16	0.056	205.51	186.69	-12.70	0.059
25	205.70	225.62	215.67	214.275	12.31	0.057	202.93	180.01	-13.73	0.064
35	206.65	228.01	216.90	214.34	12.60	0.058	200.67	176.11	-14.22	0.064
45	207.62	232.43	219.72	215.19	12.55	0.058	197.95	168.69	-15.41	-0.071

Table 3: Transformation temperatures and thermodynamic parameters of 560MPa pressure applied sample with different heating/cooling rates (5, 15, 25, 35 and 45 ˚C/min).

Heating/ cooling rate (˚C/min.)	A_s (˚C)	A_f (˚C)	A_{max} (˚C)	T_0 (˚C)	$\Delta H_{M\rightarrow A}$ (J/g)	$\Delta S_{M\rightarrow A}$ (J/g(˚C)	M_s (˚C)	M_f (˚C)	$\Delta H_{A\rightarrow M}$ (J/g)	$\Delta S_{A\rightarrow M}$ (J/g˚C)
5	174.96	184.22	180.17	180.5	2.46	0.013	176.78	167.24	-2.28	-0.012
15	174.01	187.80	180.52	180.145	2.64	0.014	172.49	146.88	-2.82	-0.015
25	173.75	191.15	181.85	180.5	2.80	0.015	169.85	158.83	-4.79	-0.026
35	175.76	195.73	184.91	181.665	3.10	0.017	167.60	136.11	-3.77	-0.020
45	185.44	225.07	206.81	195.255	1.28	0.006	165.44	143.72	-1.78	-0.009

Table 4: Transformation temperatures and thermodynamic parameters of 840 MPa pressure applied sample with different heating/cooling rates (5, 15, 25, 35 and 45 ˚C/min).

Heating/ cooling rate (˚C/min.)	A_s (˚C)	A_f (˚C)	A_{max} (˚C)	T_0 (˚C)	$\Delta H_{M\rightarrow A}$ (J/g)	$\Delta S_{M\rightarrow A}$ (J/g(˚C)	M_s (˚C)	M_f (˚C)	$\Delta H_{A\rightarrow M}$ (J/g)	$\Delta S_{A\rightarrow M}$ (J/g˚C)
5	-	-	-	-	-	-	-	-	-	-
15	-	-	-	-	-	-	-	-	-	-
25	-	-	-	-	-	-	-	-	-	-
35	306.84	358.27	339.90	270.36	3.81	0.014	182.45	158.91	-2.78	-0.010
45	392.98	437.24	415.82	312.735	10.52	0.033	188.23	160.34	-6.72	-0.021

The activation energies of the samples calculated by Kissinger method and the activation energy curve of the samples is given in Fig. 11. The calculated activation energy values of samples according to Kissinger method are processed by the following equation [19];

$$d\left[\ln\left(\varphi / T_m^2\right)\right] \Big/ d\left(1/T_m\right) = -E/R \qquad (3)$$

where ϕ is the heating rate, T_m the maximum temperature of the DSC peak, R is the universal gas constant and E is the activation energy. The calculated activation energy values for homogenous sample, 280 MPa pressure applied sample, 560MPa pressure applied sample and 840 MPa pressure applied sample are; 143.49, 43.515, 81.635 and 2.203 kJ/mol, respectively.

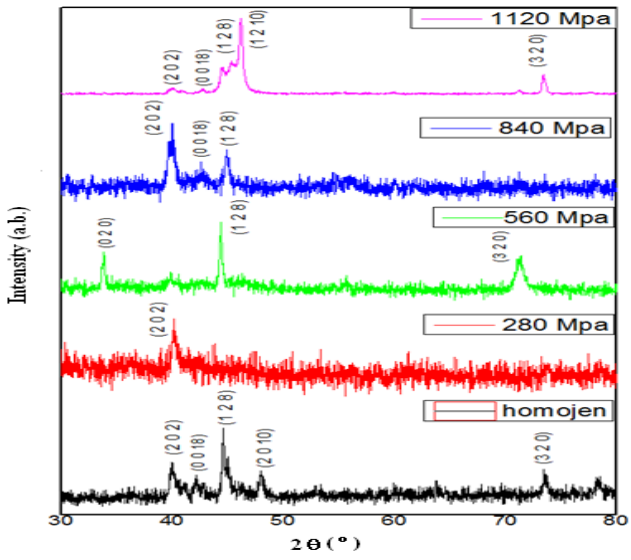

Fig. 6: *X-Ray diffraction patterns of the homogenous and pressure applied samples.*

The X-ray analysis of the homogenous sample and the pressure applied samples were made by CuK$_\alpha$ radiation at room temperature. The diffraction patterns belong to martensite phase at room temperature. As seen from X-ray results in Fig. 6, when the pressure value increased the separation of the phases became very hard. And also this was supported by the optical micrograph observations given in Fig. 7. Martensite variants, grains and grain boundries occured in the structure of the samples are clear and the orientations of martensite variants of each grain is different from each other. For the 1120MPa pressure applied sample there is no martensite variant formation and also the sample is austenite at room temperature.

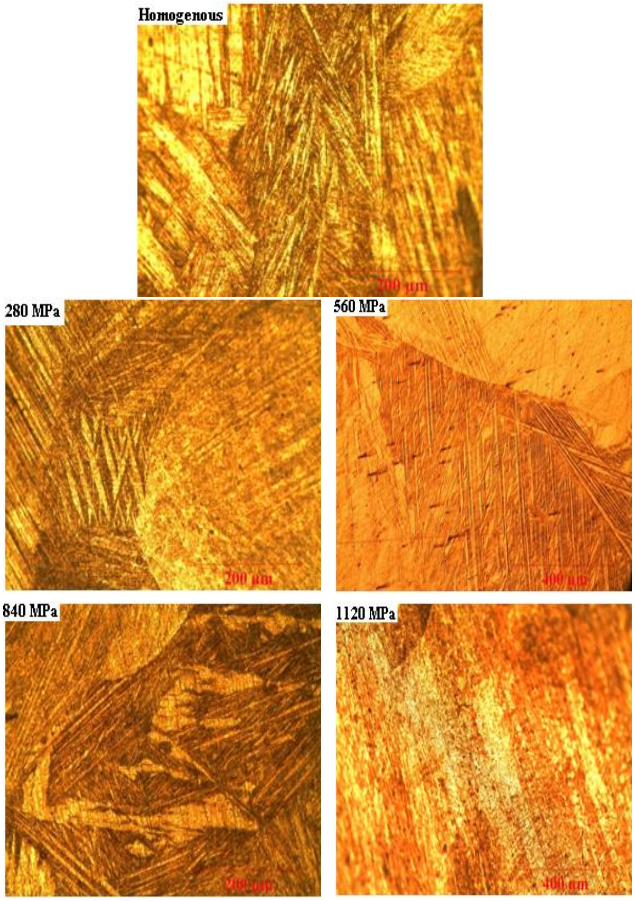

Fig. 7: *Optical micrographs of the homogenous and pressure applied samples.*

Conclusions

In this research study, we investigate the effect of increasing pressure value on the characteristic transformation temperatures and morphology of the CuAlNi SMA. As a result of the thermal and structural analysis, the increase in pressure value also increased the transformation temperatures and for the 1120MPa pressure the sample became austenite . This was both observed from thermal analysis and optical micrograph observations. In X-ray analysis for the 1120 MPa pressure the separation of the phases not occurred clearly. So, the big pressure applied on the sample deforms the structure.

References:

1] G.B. Narasimha et al., Effect of zirconium on the properties of polycrystalline Cu-Al-Be shape memory alloy. Materials Science and Engineering: A Vol. 755, 7, (2019), Pages 211-219.

[2] Miyazaki S. Development and characterization of shape memory alloys. Shape memory alloys, vol. 351. Vienna: Springer Vienna; 1996. p. 69–147.

[3] Otsuka K, Wayman C. Shape memory materials. Cambridge University Press; 1998. xiii-5.

[4]Montecinos, S., Cuniberti, A., Sepulveda, A.: Grain size and pseudoelastic behaviour of a Cu–Al–Be alloy. Mater. Charact. 59, (2008):pp.117–123.

[5]Song, G., Ma, N., Li, H.-N.: Applications of shape memory alloys in civil structures. Eng. Struct. 28, 1266–1274 (2006)

[6] Dasgupta R. A look into Cu-based shape memory alloys: present scenario and future prospects. J Mater Res 2014;29(16):1681–98.

[7] O.Karaduman and et al., Production and Characterization of Ternary Heusler Alloy with A New Composition. JMED 2(1):16-19.http://www.dergi fytronix.com/index.php/jmed/article/download/24/19

[8] J.M. Jani et al., A review of shape memory alloy research, applications and opportunities. Mater Des 2014; 56:1078–113.

[9] K. Otsuka, X. Ren, Recent developments in the research of shape memory alloys, Intermetallics 7 (1999) 511–528.

[10] J. Font, E. Cesari, J. Muntasell, J. Pons, Thermomechanical cycling in Cu–Al–Ni based melt-spun shape-memory ribbons, Mater. Sci. Eng. A 354 (2003): 207–211.

[11] S. Najah Saud Al-Humairi, Cu-Based Shape Memory Alloys: Modified Structures and Their Related Properties. Chapter in book: Recent Advances in Engineering Materials and Metallurgy Recent Advances in Engineering Materials and Metallurgy. (2019).
DOI: http://dx.doi.org/10.5772/intechopen.86193

[12] K. Sugimoto, K. Kamei, M. Nakaniwa, Cu-Al-Ni-Mn: a new shape memory alloy for high temperature applications, in: T.W. Duerig, K.N. Melton, D. Stöckel, C.M. Wayman (Eds.), Engineering Aspects of Shape Memory Alloys, Butterworth-Heinemann Ltd, London 1990, pp. 89–95.

[13] G.N. Sure, L.C. Brown, The mechanical properties of grain refinded beta-CuAlNi strain-memory alloys, Metall. Trans. A. 15A (1984) 1613–1621.

[14] K. Mukunthan, L.C. Brown, Preparation and properties of fine grain beta-CuAlNi strain-memory alloys, Metall. Trans. A. 19A (1988) 2921–2929.

[15] T. Gustmann et al., Selective laser remelting of an additively manufactured Cu-Al-Ni-Mn shape-memory alloy. Materials and Design 153, (2018): 129–138.

[16]. C.A. Canbay, et al.. Heat treatment and quenching media effects on the thermodynamical, thermoelastical and structural characteristics of a new Cu-based quaternary shape memory alloy. Composites Part B 174 (2019) 106940. DOI: 10.1016/j.compositesb.2019.106940

[17] R.A.Portier, P.Ochin, A.Pasko, G.E.Monastyrsky, A.V.Gilchuk, V.I.Kolomytsev, Y.N.Koval, Spark plasma sintering of Cu-Al-Ni shape memory alloy, J Alloy Compd. Article in press.

[18] M.O. Prado, P.M. Decarte, F. Lovey, Martensitic transformation in Cu-Mn-Al alloys, ScriptaMetall. Mater. 33 (1995) 878-83.

[19] H.E. Kissinger, Reaction Kinetics in Differential Thermal Analysis, Anal. Chem. 29-11 (1957)1702-1706

[20] Y.Sutou, R. Kainuma, K. Ishida, Effect of alloying elements on the shape memory properties of ductile Cu-Al-Mn alloys, Mater. Sci. Eng. A 273-275 (1999) 375-379.

[21] U.S. Mallik, V. Sampath, Influence of quaternary alloying additions on transformation temperatures and shape memory properties of Cu-Al-Mn shape memory alloy, J. Alloys Compd. 469 (2009) 156-163.

[22] J. Fernandez, A.V. Benedetti, J.M. Guilemany, X.M. Zhang, Thermal stability of the martensitic transformation of Cu-Al-Ni-Mn-Ti, Mater. Sci. Eng. A 438-440 (2006) 723-725.

**